Tunable interaction-free all-optical switching in a five-level atom-cavity system

Tiantian Liu (刘甜甜), Gongwei Lin (林功伟)*, Fengxue Zhou (周凤雪), Li Deng (邓 立), Shangqing Gong (龚尚庆), and Yueping Niu (钮月萍)

College of Physics, East China University of Science and Technology, Shanghai 200237, China
**Corresponding author: gwlin@ecust.edu.cn*

Received March 31, 2017; accepted May 25, 2017; posted online June 21, 2017

A scheme is proposed for tunable all-optical switching based on the double-dark states in a five-level atom-cavity system. In the scheme, the output signal light of the reflection and the transmission channels can be switched on or off by manipulating the control field. When the control light is coupled to the atom-cavity system, the input signal light is reflected by the cavity. Thus, there is no direct coupling between the control light and the signal light. Furthermore, the position of the double-dark states can be changed by adjusting the coherent field, and, thus, the switching in our scheme is tunable. By presenting the numerical calculations of the switching efficiency, we show that this type of the interaction-free all-optical switching can be realized with high switching efficiency.

OCIS codes: 270.1670, 230.1150, 190.4180.
doi: 10.3788/COL201715.092702.

With the development of optical communications and quantum information network, the all-optical switching, in which a signal light beam can be fully controlled by a control light field, has attracted a lot of attention in recent years[1–14]. Particularly, with the optical nonlinearities, schemes of interaction-free all-optical switching have been proposed and demonstrated[15–19]. In these interaction-free schemes, it is possible to eliminate the direct coupling between the signal light and the control light. Then, the signal photon loss in the absorbing medium is suppressed. However, these schemes[15–19] are limited by the achievable optical nonlinearities for low light intensities.

Recently, Zou *et al.*[20] proposed a new method for interaction-free all-optical switching based on three-level atoms confined in an optical cavity. They showed that with the quantum interference effect[8,21–23], a weak control light can be used to suppress the normal-mode excitation from the signal light. Thus, the interaction-free all-optical switching would be operated at low light intensities. In this Letter, we present an alterable scheme for interaction-free all-optical switching based on the quantum interference effect[8,21–23]. In our scheme, we use the double-dark states[24–26] in the five-level atom-cavity system to realize the optical switching. As the dark state does not contain the excited states, the switching in our scheme is not affected by the spontaneous emission and can be realized with higher switching efficiencies, compared to the previous scheme[20]. What is more, the frequency position of the double-dark states can be changed by adjusting the coherent field; thus, the switching in our system is tunable.

We consider a composite atom-cavity system that consists of a single mode cavity containing N five-level atoms, as shown in Fig. 1. Each atom contains three ground states $|1\rangle$, $|3\rangle$, $|4\rangle$ and two excited states $|2\rangle$, $|5\rangle$. The cavity mode and a pump laser resonantly couple the atomic transitions $|1\rangle \to |2\rangle$ and $|2\rangle \to |3\rangle$ with the coupling strengths g and Ω_1, respectively. The twofold levels, labeled 3 and 4, are coupled by a coherent field with the Rabi frequency Ω_2, which can be a microwave or quasi-static field[26]. These four states coupled by the cavity mode and two coherent fields constitute a four-level electromagnetic induced transparence (EIT) system, which contains the double-dark state structure[25]. In addition, the cavity mode is driven by a signal field ξ_p with frequency detuning $\Delta_p = \omega_p - \omega_a$; here, ω_p is the frequency of the signal field, and ω_a is the eigenfrequency of the cavity mode. A free-space control laser Ω_3 drives the atomic transition $|4\rangle \to |5\rangle$ with frequency detuning $\Delta = \omega_3 - \omega_{54}$, where ω_3 is the frequency of the control laser, and ω_{54} is the transition frequency between states $|5\rangle$ and $|4\rangle$. The Hamiltonian of the system can be written as

$$\begin{aligned} H = & \sum_{k=1}^{N} \Delta |5\rangle_k\langle 5| \\ & + \sum_{k=1}^{N} (g a^\dagger \sigma_{12}^{(k)} + \Omega_1 \sigma_{23}^{(k)} + \Omega_2 \sigma_{34}^{(k)} + \Omega_3 \sigma_{54}^{(k)} + \text{H.c.}) \\ & + i(\xi_p a^\dagger e^{-i\Delta_p t} - \xi_p^* a e^{i\Delta_p t}), \end{aligned} \tag{1}$$

where a ($a^\dagger$) is the annihilation (creation) operator of the cavity mode, and $\sigma_{lm}^{(k)} = |l\rangle_k\langle m|(l, m = 1\text{–}5)$ is the atomic transition operator for the kth atom. ξ_p is related to the laser power P by $\xi_p = \sqrt{(2\kappa P/\hbar\omega_p)}$, where κ denotes the cavity decay rate. Define the collective operator of the atoms $S_p^\dagger = \frac{1}{\sqrt{N}} \sum_{k=1}^{N} |p\rangle_k\langle 1|$ with $p = 2, 3, 4, 5$. Then, the Hamiltonian H can be represented by

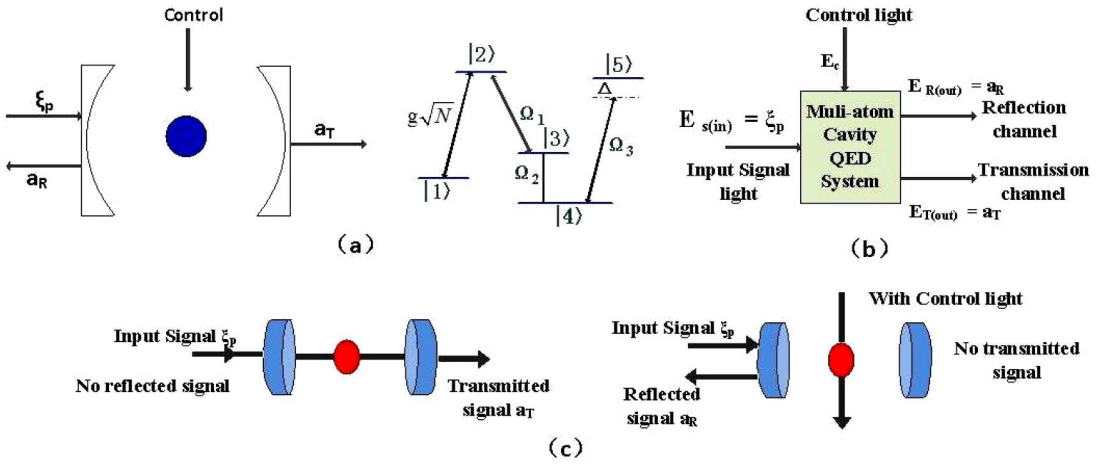

Fig. 1. (a) Schematic diagram for the tunable interaction-free all-optical switching in a five-level atom-cavity system. (b) The schematic diagram of the input–output channels. (c) The detailed output states of the all-optical switching. When there is no control light, there is output signal light from the transmission channel, but no light from the reflection channel; when the control light is on, the signal light cannot be coupled into the cavity, the output is switched to the reflection channel, and there is no output light from the transmission channel. There is no direct coupling between the signal light and the control light.

$$\begin{aligned} H =& \Delta S_5^\dagger S_5 + g\sqrt{N}(a^\dagger S_2 + S_2^\dagger a) + \Omega_1(S_2^\dagger S_3 + S_3^\dagger S_2) \\ &+ \Omega_2(S_3^\dagger S_4 + S_4^\dagger S_3) + \Omega_3(S_4^\dagger S_5 + S_5^\dagger S_4) \\ &+ i(\xi_p a^\dagger e^{-i\Delta_p t} - \xi_p^* a e^{i\Delta_p t}). \end{aligned} \tag{2}$$

Considering photon losses from the cavity and the decays of the atoms, the dynamic equations of the system are given in a rotating frame by the quantum Langevin equations,

$$\dot{a} = -(i\Delta_p + \kappa)a - ig\sqrt{N}S_2 + \xi_p + \sqrt{2\kappa}a_{\rm in}(t), \tag{3a}$$

$$\dot{S}_2 = -\left(i\Delta_p + \frac{\gamma_2}{2}\right)S_2 - ig\sqrt{N}a - i\Omega_1 S_3 + \sqrt{\gamma_2}\zeta_2(t), \tag{3b}$$

$$\dot{S}_3 = -i\Delta_p S_3 - i\Omega_1 S_2 - i\Omega_2 S_4, \tag{3c}$$

$$\dot{S}_4 = -i\Delta_p S_4 - i\Omega_2 S_3 - i\Omega_3 S_5, \tag{3d}$$

$$\dot{S}_5 = -\left[i(\Delta_p - \Delta) + \frac{\gamma_5}{2}\right]S_5 - i\Omega_3 S_4 + \sqrt{\gamma_5}\zeta_5(t), \tag{3e}$$

where $\gamma_i (i = 2, 5)$ denotes the decay rate of the atom. Here, we have ignored the decoherence rates between the ground states. $a_{\rm in}(t)$ and $\zeta_i(t)$ with zero mean values denote the input vacuum noises associated with the cavity mode and the atomic system, respectively. They obey the nonvanishing commutation relations[27] $\langle a_{\rm in}(t)a_{\rm in}^\dagger(t')\rangle = \delta(t-t')$ and $\langle \zeta_i(t)\zeta_i^\dagger(t')\rangle = \delta(t-t')$. Under the mean-field approximation $\langle Qc\rangle = \langle Q\rangle\langle c\rangle$[28], the mean value equations are given by

$$\langle \dot{a}\rangle = -(i\Delta_p + \kappa)\langle a\rangle - ig\sqrt{N}\langle S_2\rangle + \xi_p, \tag{4a}$$

$$\langle \dot{S}_2\rangle = -\left(i\Delta_p + \frac{\gamma_2}{2}\right)\langle S_2\rangle - ig\sqrt{N}\langle a\rangle - i\Omega_1\langle S_3\rangle, \tag{4b}$$

$$\langle \dot{S}_3\rangle = -i\Delta_p\langle S_3\rangle - i\Omega_1\langle S_2\rangle - i\Omega_2\langle S_4\rangle, \tag{4c}$$

$$\langle \dot{S}_4\rangle = -i\Delta_p\langle S_4\rangle - i\Omega_2\langle S_3\rangle - i\Omega_3\langle S_5\rangle, \tag{4d}$$

$$\langle \dot{S}_5\rangle = -\left[i(\Delta_p - \Delta) + \frac{\gamma_5}{2}\right]\langle S_5\rangle - i\Omega_3\langle S_4\rangle. \tag{4e}$$

In this section, we show the tunable interaction-free all-optical switching based on the five-level atom-cavity system. Without loss of generality, we assume that $\gamma_2 = \gamma_5 = \gamma$. Then, the steady-state solution of the system is given by

$$\langle a\rangle = \frac{\xi_p}{i\Delta_p + \kappa + \dfrac{g^2 N}{i\Delta_p + \frac{\gamma}{2} + \dfrac{\Omega_1^2}{i\Delta_p + \dfrac{\Omega_2^2}{i\Delta_p + \dfrac{\Omega_3^2}{i(\Delta_p - \Delta) + \frac{\gamma}{2}}}}}}. \tag{5}$$

In this system, the input signal light is coupled into the cavity and results in two output channels: the reflected signal light from the cavity and the transmitted signal light though the cavity. The reflected signal field from the cavity is given by[20] $a_R = \sqrt{2\kappa}\langle a\rangle - \xi_p$, and the transmitted signal field through the cavity is given by $a_T = \sqrt{2\kappa}\langle a\rangle$. The schematic diagram of the input–output channels are showed in Fig. 1(b). The states of the two output channels are controlled by the free-space control light Ω_3. Figure 1(c) shows the detailed output states.

In Fig. 2, we plot the reflected signal light intensity $I_R = a_R^* a_R$ and the transmitted signal light intensity

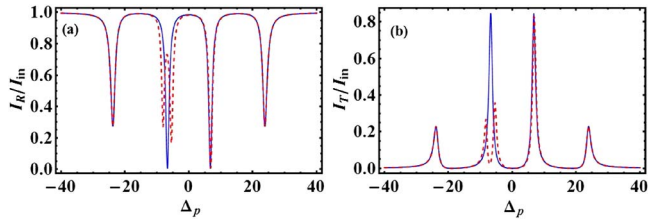

Fig. 2. (Color online) (a) Reflected signal intensity ($I_R/I_{\rm in}$) and (b) the transmitted signal intensity ($I_T/I_{\rm in}$) as functions of the frequency detuning of the signal field Δ_p. Solid blue line, $\Omega_3 = 0$ MHz; dashed red line, $\Omega_3 = 2$ MHz. The rest of the parameters are $g\sqrt{N} = 16$ MHz, $\xi_p = 2$ MHz, $\gamma = 1$ MHz, $\kappa = 2$ MHz, $\Omega_1 = 16$ MHz, and $\Omega_2 = 10$ MHz.

$I_T = a_T^* a_T$ normalized by the input signal intensity $I_{\rm in} = |\xi_p|^2$ versus the signal laser detuning Δ_p. From the solid blue line in Fig. 2(a), one can observe that when the control laser is absent ($\Omega_3 = 0$), there are two deep dips in the middle of the reflected signal spectrum. Correspondingly, there are two high peaks in the middle of the transmitted signal spectrum, as shown in Fig. 2(b) (solid blue line). The two dips/peaks represent the double-dark states in frequency $\pm d$ with $d = \sqrt{\frac{g^2N+\Omega_1^2+\Omega_2^2-\sqrt{(g^2N+\Omega_1^2+\Omega_2^2)^2-4g^2N\Omega_2^2}}{2}}$. The double-dark states do not contain the excited states and are nearly unaffected by the spontaneous emission. The two lower dips/peaks beside the double-dark states in Fig. 2 are the bright states, which contain the excited states with large spontaneous emission.

The dashed red lines in Figs. 2(a) and 2(b) plot the reflection and transmission spectrum when the control laser with frequency detuning $\Delta = -d$ is present ($\Omega_3 \neq 0$). The spectrum show that at dark-state resonance ($\Delta_p = -d$), as the control laser field induces destructive interference, the transmitted signal light is suppressed, while the reflected signal light is maximized. Therefore, the control laser can be used to switch the signal light. So, the coupled atom-cavity system can be used to perform an all-optical switching controlled by a weak control light Ω_3. When the control laser is coupled to the system, the signal light cannot be coupled into the cavity and, then, is reflected from the cavity. Therefore, the all-optical switching is performed without the direct coupling between the control light and the signal light, and, thus, it is interaction free.

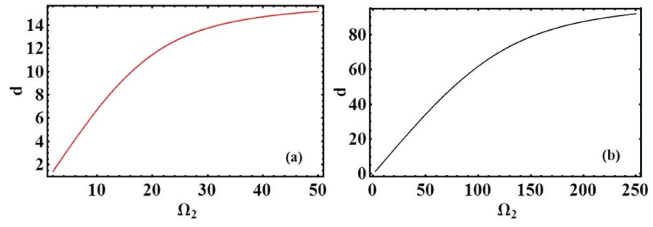

Fig. 3. Resonant frequency of the dark state as function of the coherent intensity Ω_2. Other parameters are (a) $g\sqrt{N} = 16$ MHz and $\Omega_1 = 16$ MHz and (b) $g\sqrt{N} = 100$ MHz and $\Omega_1 = 100$ MHz.

We plot the resonant frequency d of the dark state versus the coherent field Ω_2 in Fig. 3. From Fig. 3, we can see that the resonant frequency d of the dark state is a monotonically increasing function of Ω_2 and is saturated at a moderate Ω_2 value. That is to say, the position of the double-dark states can be manipulated by adjusting the intensity of the coherent field. With a large $g\sqrt{N}$ value ($g\sqrt{N} = 100$ MHz), we can get a large tunable range, as shown in Fig. 3(b). As shown in the experiment, $g\sqrt{N}$ would reach to 190 MHz even in the low quality cavity with many atoms[29]. Hence, the optical switching in our scheme would be tunable in a large range.

Next, we analyze the efficiencies of the interaction-free all-optical switching. From Fig. 2, one can see that when the control light is present, the signal light is reflected from the cavity (the reflection channel is opened), while the transmitted light through the cavity is suppressed (the transmission channel is closed). When the control light is absent, the transmission channel is opened, and the reflection channel is closed. Following the method in Ref. [20], one can obtain the switching efficiency of the reflection output channel and the transmission output channel: $\eta_{R/T} = \frac{I(o)-I(c)}{I_{\rm in}}$. Here, $I(o)$ is the signal output intensity when the switching is opened, $I(c)$ is the signal output intensity when the switching is closed $[I(o) > I(c)]$, and $I_{\rm in}$ is the input signal intensity.

Figures 4–6 show the switching efficiencies η_R and η_T versus the parameters $g\sqrt{N}$, Ω_3, Ω_1, and Ω_2, separately. From Fig. 4, one can see that η_R and η_T are monotonically increasing functions of $g\sqrt{N}$ and are saturated at moderate $g\sqrt{N}$ values. This means that the high efficiency depends on a moderately large coupling coefficient $g\sqrt{N}$. Figure 5 shows that the interaction-free all-optical switching in the cavity-atom system can be done with a relatively weak control laser. The switching efficiency (especially η_T) increases rapidly with the increasing control field, but saturates at Ω_3 values smaller than other parameters, like $g\sqrt{N}$ and Ω_2. This is similar to the figures in the three-level atom-cavity system[20]. Figure 6 plots η_R and η_T versus the pump field Ω_1 and the coherent field Ω_2. It shows that the pump field Ω_1 and the coherent field Ω_2 have little

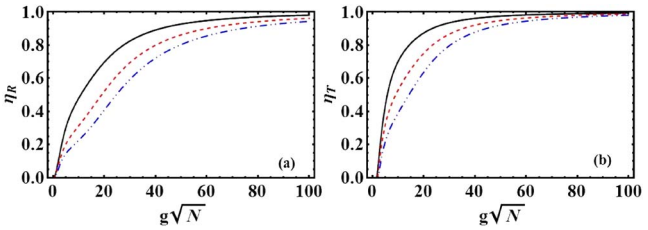

Fig. 4. (Color online) Switching efficiencies of (a) the reflected output field η_R and (b) the transmitted output field η_T versus the atom-cavity coupling $g\sqrt{N}$ with $\gamma = 1$ MHz (black solid lines), $\gamma = 2$ MHz (red dashed lines), and $\gamma = 3$ MHz (blue dotted lines), respectively. Other parameters are $\xi_p = 2$ MHz, $\kappa = 3$ MHz, $\Omega_1 = 16$ MHz, $\Omega_2 = 10$ MHz, $\Omega_3 = 2$ MHz, and $\Delta_p = \Delta = -d$.

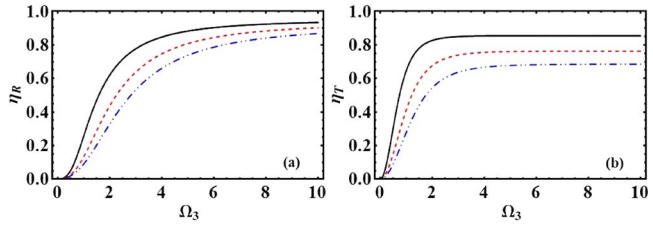

Fig. 5. (Color online) Switching efficiencies of (a) the reflected output field η_R and (b) the transmitted output field η_T versus the control field Ω_3 with $\gamma = 1$ MHz (black solid lines), $\gamma = 2$ MHz (red dashed lines), and $\gamma = 3$ MHz (blue dotted lines), respectively. Other parameters are $\Delta_p = \Delta = -d$ MHz, $\xi_p = 2$ MHz, $\kappa = 3$ MHz, $g\sqrt{N} = 16$ MHz, $\Omega_2 = 10$ MHz, and $\Omega_1 = 16$ MHz.

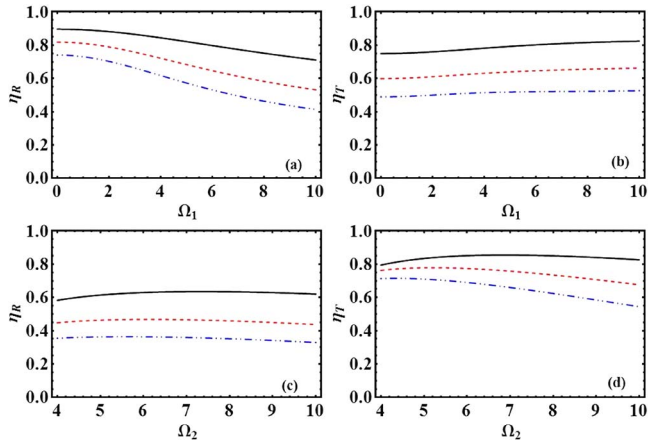

Fig. 6. (Color online) Switching efficiencies of (a) the reflected output field η_R and (b) the transmitted output field η_T versus the pump field Ω_1 with $\gamma = 1$ MHz (black solid lines), $\gamma = 2$ MHz (red dashed lines), and $\gamma = 3$ MHz (blue dotted lines), respectively. Other parameters are $\Delta_p = \Delta = -d$ MHz, $\xi_p = 2$ MHz, $\kappa = 3$ MHz, $g\sqrt{N} = 16$ MHz, $\Omega_2 = 10$ MHz, and $\Omega_3 = 2$ MHz. (c) η_R and (d) η_T versus the coherent field Ω_2 with $\gamma = 1$ MHz (black solid lines), $\gamma = 2$ MHz (red dashed lines), and $\gamma = 3$ MHz (blue dotted lines), respectively. Here, $\Omega_1 = 16$ MHz, and other parameters are the same as (a) and (b).

impact on the switching efficiency. From Figs. 4–6, one can find that the switching efficiency decreases with the increasing of the atom decay rate γ.

Finally, we address the experimental feasibility of the present scheme. The atomic configuration can be chosen from the hyperfine states of the Rb atoms ($\gamma = 3$ MHz). The atoms are confined in a 5 cm cavity with a finesse of 150 ($\kappa = 10$ MHz) with $g\sqrt{N} = 50$ MHz ($N \approx 10^4$ atoms). We choose the parameters $\Omega_3 = 1.5$ MHz, $\Omega_2 = 6$ MHz, and $\Omega_1 = 5$ MHz, and the switching efficiency is derived to be $\eta_R = 0.86$ and $\eta_T = 0.98$. Compared with the switching efficiency in Ref. [20] with $\eta_R = 0.83$ and $\eta_T = 0.56$ under the same parameters of the cavity and the intensity of the control field, there is little difference between the reflection efficiency η_R, but the transmission efficiency η_T is greatly enhanced in our scheme. This is because in Ref. [20], the switching is realized based on the bright states, which contain the excited states. Thus, the transmitted light through the cavity is greatly influenced by the spontaneous emission. However, in our scheme, the switching is achieved based on the double-dark states, which do not contain the excited states and are nearly unaffected by the spontaneous emission. Therefore, the switching efficiency of the transmission channel is much higher than that in Ref. [20].

In conclusion, we demonstrate a tunable interaction-free all-optical switching in a five-level atom-cavity system. Compared with the interaction-free all-optical switching in the three-level atom-cavity system[20], we utilize the double-dark states rather than the bright states to realize the all-optical switching; thus, the switching efficiency is greatly improved. What is more, the position of the double-dark states can be changed by adjusting the coherent interaction, so the switching in our system is tunable.

This work was supported by the National Natural Sciences Foundation of China (Nos. 11674094, 11274112, 91321101, and 61275215) and the Fundamental Research Funds for the Central Universities (No. WM1313003).

References

1. S. E. Harris and Y. Yamamoto, Phys. Rev. Lett. **81**, 3611 (1998).
2. A. M. C. Dawes, L. Illing, S. M. Clark, and D. J. Gauthier, Sci.: Int. Ed.–AAAS **308**, 672 (2005).
3. T. Tanabe, M. Notomi, S. Mitsugi, A. Shinya, and E. Kuramochi, Appl. Phys. Lett. **87**, 151112 (2005).
4. J. Zhang, G. Hernandez, and Y. Zhu, Opt. Lett. **32**, 1317 (2007).
5. M. Bajcsy, S. Hofferberth, V. Balic, T. Peyronel, M. Hafezi, A. S. Zibrov, V. Vuletic, and M. D. Lukin, Phys. Rev. Lett. **102**, 203902 (2009).
6. J. Scheuer, A. A. Sukhorukov, and Y. S. Kivshar, Opt. Lett. **35**, 3712 (2010).
7. F. Qin, Y. Liu, Z.-M. Meng, and Z.-Y. Li, J. Appl. Phys. **108**, 053108 (2010).
8. X. Wei, J. Zhang, and Y. Zhu, Phys. Rev. A **82**, 033808 (2010).
9. M. Albert, A. Dantan, and M. Drewsen, Nat. Photon. **5**, 633 (2011).
10. B. Zou and Y. Zhu, Phys. Rev. A **87**, 053802 (2013).
11. J. Liu, L. Xue, G. Kai, and X. Dong, Chin. Opt. Lett. **5**, S214 (2007).
12. Y. Shen, G. Yu, J. Fu, and L. Zou, Chin. Opt. Lett. **10**, 021301 (2012).
13. N. Wada, B. J. Puttnam, R. S. Luis, W. Klaus, J. Sakaguchi, J. M. D. Mendinueta, Y. Awaji, S. Shinada, and H. Furukawa, Chin. Opt. Lett. **12**, 120004 (2016).
14. H. Qiu, Z. Wu, T. Deng, Y. He, and J. Xia, Chin. Opt. Lett. **14**, 021401 (2016).
15. B. C. Jacobs and J. D. Franson, Phys. Rev. A **79**, 063830 (2009).
16. Y. Huang and P. Kumar, Opt. Lett. **35**, 2376 (2010).
17. Y. P. Huang, J. B. Altepeter, and P. Kumar, Phys. Rev. A **82**, 063826 (2010).
18. K. T. McCusker, Y.-P. Huang, A. S. Kowligy, and P. Kumar, Phys. Rev. Lett. **110**, 240403 (2013).
19. S. M. Hendrickson, C. N. Weiler, R. M. Camacho, P. T. Rakich, A. I. Young, M. J. Shaw, T. B. Pittman, J. D. Franson, and B. C. Jacobs, Phys. Rev. A **87**, 023808 (2013).
20. B. Zou, Z. Tan, M. Musa, and Y. Zhu, Phys. Rev. A **89**, 023806 (2014).
21. J. Zhang, G. Hernandez, and Y. Zhu, Opt. Express **16**, 7861 (2008).

22. Y. Zhu, Opt. Lett. **35**, 303 (2010).
23. M. D. Lukin, M. Fleischhauer, M. O. Scully, and V. L. Velichansky, Opt. Lett. **23**, 295 (1998).
24. B. Y. Chang, I. R. Solá, V. S. Malinovsky, and J. Santamaría, Phys. Rev. A **64**, 033420 (2001).
25. M. D. Lukin, S. F. Yelin, M. Fleischhauer, and M. O. Scully, Phys. Rev. A **60**, 3225 (1999).
26. Y. Niu, S. Gong, R. Li, and S. Jin, Phys. Rev. A **70**, 023805 (2004).
27. M. J. Akram, F. Saif, and F. Ghafoor, J. Phys. B: At. Mol. Opt. Phys. **48**, 065502 (2015).
28. G. S. Agarwal and S. Huang, Phys. Rev. A **81**, 041803 (2010).
29. H. Wu, J. Gea-Banacloche, and M. Xiao, Phys. Rev. Lett. **100**, 173602 (2008).